

SIGE BIPOLAR JUNCTION TRANSISTORS FOR MICROWAVE POWER APPLICATIONS

Gregory N. Henderson⁽¹⁾, Matthew F. O'Keefe⁽¹⁾, Timothy E. Boles⁽²⁾, Paulette Noonan⁽²⁾, John M. Sledziewski⁽²⁾, and Brian M. Brown⁽²⁾

⁽¹⁾*Corporate R&D*

⁽¹⁾*Semiconductor Business Unit*

M/A-COM

*100 Chelmsford Street,
Lowell, MA 01851-2694*

ABSTRACT:

High-efficiency silicon germanium (SiGe) bipolar junction transistors have been developed for 5-10V, 1.88GHz power amplifier applications. Class A-B biased common base parts have demonstrated a power gain $G_p=16\text{dB}$, one-dB compression point $P_{1\text{dB}}=25\text{dBm}$ and power-added-efficiency PAE($P_{1\text{dB}}$)=53% at $V_c=5\text{V}$ and >1W output power with >15dB gain and >50% PAE at $V_c=10\text{V}$. Common-emitter measurements ($V_c=7\text{V}$) have demonstrated an output power of 28dBm with greater than 60% collector efficiency. Under two-tone operation, the devices have achieved an output power of 23dBm with 37% PAE at a third-order-intermodulation distortion of IM3=30dBc. These results represent a significant improvement over conventional Si BJT's.

INTRODUCTION:

SiGe devices have attracted recent attention for a variety of wireless communications applications including transceivers, oscillators, and power devices [1-3]. SiGe BJT's have been demonstrated for power applications at 900MHz with >70% PAE, and at 2GHz with 45% PAE [2]. This paper describes the design, growth, and fabrication of high efficiency SiGe BJT's for power applications at 1.88GHz. The devices developed here have demonstrated (at $P_o\sim24\text{-}30\text{dBm}$) excellent gain (>15dB) and power-added efficiency (>50%) for Si devices at 1.88GHz; the performance rivaling that of GaAs FET's and HBT's at this frequency. Further, under 2-tone operation, the devices have demonstrated a significant improvement in PAE (at the same linearity) over conventional Si BJT's.

DEVICE DESIGN, GROWTH, AND FABRICATION:

In order to be used in 5V power applications, the collector epitaxy was designed to have $V_{ceo} > 9\text{-}10$ volts and $V_{cbo} > 15\text{V}$. The base and emitter doping profiles were designed to maximize f_{MAX} . To achieve this, the Ge is graded across the base in order to provide an accelerating field. The base thickness is determined to obtain an appropriate tradeoff between DC gain, f_T , f_{MAX} , and critical SiGe thickness. The simulated performance for the intrinsic (no parasitics) small-signal device (see Fig. 1 for profile) is: $V_{cbo}=15\text{V}$, $V_{ceo}=10\text{V}$, $f_T \sim 35\text{GHz}$ and $f_{\text{MAX}} \sim 35\text{GHz}$.

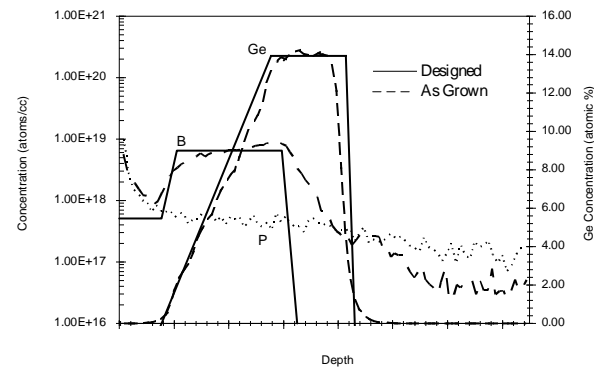


Fig. 1. SIMS data of the small-signal SiGe graded base BJT versus designed profile.

Material was grown using a hot-wall ultra high vacuum chemical vapor deposition (UHV-CVD) system using silane and germane as the source gases. N-type and p-type doping was achieved using phosphine and diborane respectively. The devices are fabricated using a double-polysilicon process, as shown in Fig. 2.

The devices are mesa isolated, with backside collector contacts. Implantations of BF_2 and phosphorus are used to define the base and emitters, respectively.

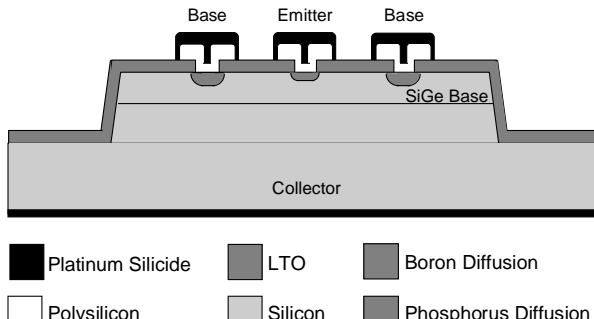


Fig. 2. A schematic of the SiGe BJT device cross-section prior to passivation and final metallization.

SMALL-SIGNAL DEVICE PERFORMANCE:

First-generation, small-signal devices were fabricated using the material profile and process shown in Figs. 1-2. The small-signal device is a 17 finger by 14 μm device with 0.6 μm wide emitter stripe and a 3.6 μm emitter-emitter pitch. Undebiased common-emitter measured small-signal characteristics are shown in Fig. 3 demonstrating a measured $f_T \sim 15\text{GHz}$ and f_{MAX} (as measured from MSG/MAG) $\sim 14\text{GHz}$. More importantly for power performance, the devices have an MSG/MAG at 2GHz $> 15\text{dB}$.

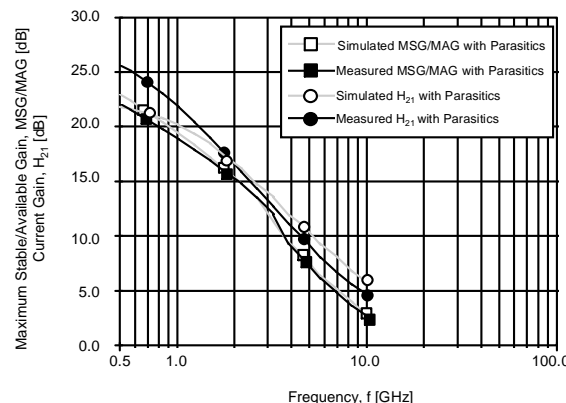


Fig. 3. Measured and simulated MSG/MAG and h_{21} at $V_c=4\text{V}$ and $I_c=90\text{mA}$ for the small signal device with $f_T=15\text{GHz}$ and $f_{\text{MAX}}=14\text{GHz}$.

Small-signal simulations were also performed using a two-dimensional physical model which was embedded inside an extracted parasitic network (Fig.4). The base, emitter, and collector bond wire inductances were extracted from measurements on dummy structures. The feedback capacitance is the parasitic base-collector mesa capacitance which is calculated from the layout. The 2.5 Ω emitter resistance and 6.4 Ω collector resistance were extracted from open collector measurements. Using these measured and extracted parasitics, the simulated performance is extremely close to the measured values (see Fig. 3).

Of the parasitics described above, the collector resistance of 6.4 Ω is anomalously high for this collector doping; models and similar Si parts indicate it should be less than 2 Ω . If one uses a collector resistance of 2 Ω and removes the bond wire parasitics from the simulation circuit shown in Fig. 4, the simulated f_T and f_{MAX} for the device are significantly higher (See Fig. 5). Further, as can be seen from the simulations in Fig. 5, the collector resistance has little effect on the gain at 2GHz, where these devices are to be used. In fact, measured load-pull power measurements for these small die show, when tuned for gain, the device has a power gain $G_p=16\text{dB}$, a one-dB compression point of $P_{1\text{dB}}=18\text{dBm}$ and a one-dB compressed power-added efficiency $\text{PAE}=29\%$. When tuned for efficiency and driven into compression, the device achieves a power gain $G_p=8\text{dB}$, $P_o=20\text{dBm}$, and $\text{PAE}=51\%$.

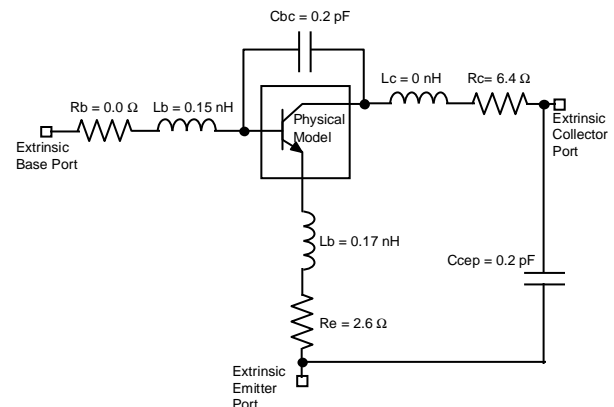


Fig. 4. Simulation circuit for modeling small-signal performance using the physical model and extracted parasitics.

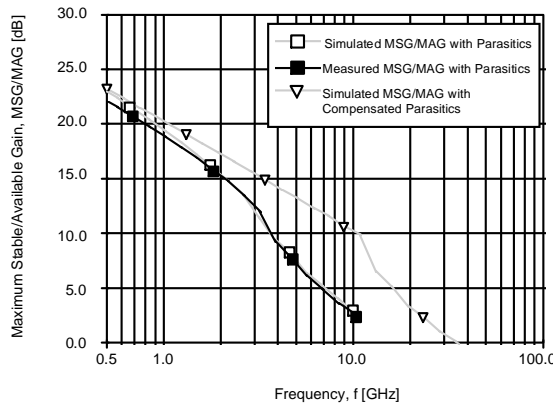


Fig. 5. Measured and simulated maximum available/stable gain at $V_c=4V$ and $I_c=90mA$, using model with compensated parasitics.

POWER DEVICE PERFORMANCE:

In order to solve the anomalous collector resistance problems, a modified epitaxial growth procedure was used to fabricate the material for the power devices. Further, these devices were designed to have a slightly higher breakdown voltage, $V_{cbo} > 20V$ and $V_{ceo} > 10V$. With the exception of the collector modifications, identical base and emitter growth and processing was used for the power devices which consist of two 46 finger $\times 21\mu m$ cells. These devices were laid out for common-base mounting - but were tested in both common-emitter and common-base configurations.

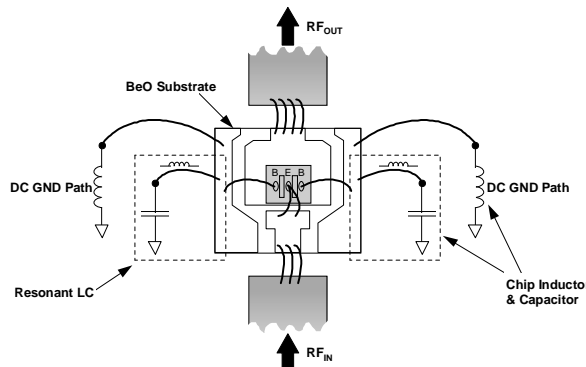


Fig. 6. Assembly configuration for power testing. The die is soldered to a BeO substrate, and a chip capacitor is used to resonate out the ground inductance. Common-base configuration is shown.

The power devices were mounted collector down on a 10 mil metallized BeO substrate which

was in turn soldered to a heat sink (see Fig. 6). The collector and emitter (base) signals were brought to the device on alumina microstrip transmission lines in common base (emitter) configuration. The base (emitter) ground inductance was resonated out using chip capacitors and bond wires. As the power-devices were unballasted, they could only be run in Class-AB and Class B operation.

The devices were measured using a computer controlled mechanical tuner load-pull stand. Figure 7 shows the measured Class AB power-sweep for a common-base mounted device at $V_c=5V$, $f=1.88GHz$; the device has a one-dB compression point ($P_{1dB}=25dBm$), a one-dB compressed gain $G=16dB$, and a one-dB compressed power-added efficiency $PAE=53\%$. At $V_c=10V$ (see Fig. 8), the device achieves $P_o=30dBm$, $G_p=17dBm$, and $PAE=50\%$.

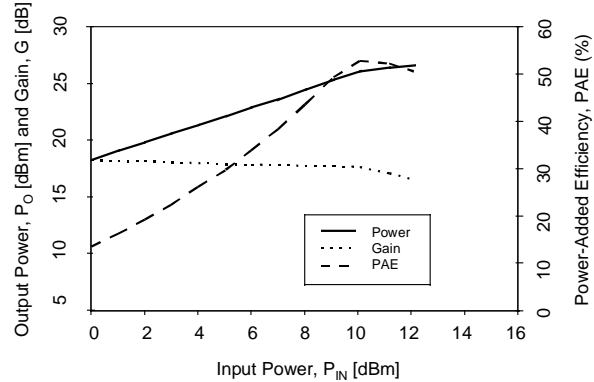


Fig. 7. Class A-B common-base power sweep of power SiGe BJT at $V_c=5V$ and $f=1.88GHz$.

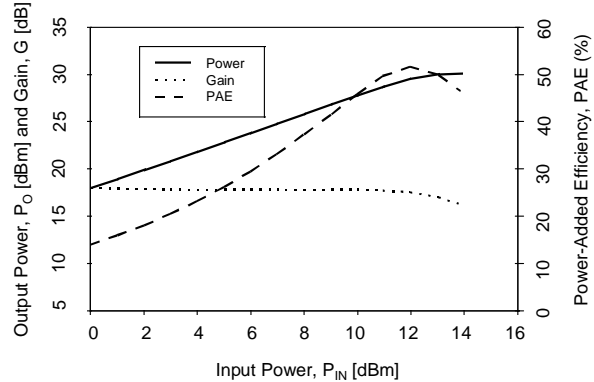


Fig. 8. Class A-B common-base power sweep of power SiGe BJT at $V_c=10V$ and $f=1.88GHz$.

As the transistors are operated in Class AB mode, a significant amount ($\sim 20\%$) of the DC input power is dissipated across the base-emitter junction ($\sim 0.8V \cdot I_c$), while the output power is limited by the swing across the base-collector junction. Thus, common-emitter mounted devices should have significantly higher PAE than the common-base counterparts. For this reason, die were mounted in common-emitter configuration with a resonant circuit used to resonate out the emitter bond wire.

As the die were laid out for common-base operation, the common-emitter gain is low due to difficulty in effectively resonating out the long emitter bond wire. Nevertheless, the results show good gain and efficiency, as shown in Fig. 9, which shows results at $V_c=7V$ tuned for both power and efficiency. Tuned for power, the device achieves $G_p=13\text{dB}$ peak gain, $P_{1\text{dB}}=29\text{dBm}$, and $\text{PAE}(P_{1\text{dB}})=40\%$; tuned for efficiency, the device achieves $\text{PAE}=52\%$ at $P_o=28\text{dBm}$. The PAE in this case is limited by the device gain; the collector efficiency being $> 60\%$. More importantly, due to the high collector efficiency, under two-tone operation the device can achieve a $\text{PAE}=37\%$, at a peak-envelope-power (PEP) of 29dBm ($P_o=23\text{dBm}$) and $\text{IM3}=30\text{dBc}$ [as shown in Fig. 10], which is a significant improvement over Si BJT's for linear applications at 1.88GHz [4]. Current efforts are directed towards improving the common-emitter match to enhance the common-emitter device gain and PAE.

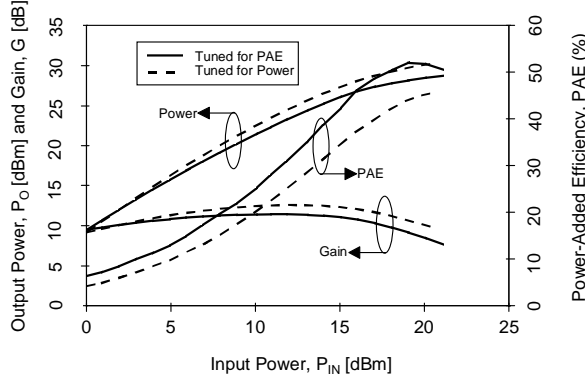


Fig. 9. Class A-B common-emitter power sweeps of SiGe BJT at $V_c=7V$ and $f=1.88\text{GHz}$. The

dashed line is tuned for maximum power and the solid line is tuned for maximum PAE.

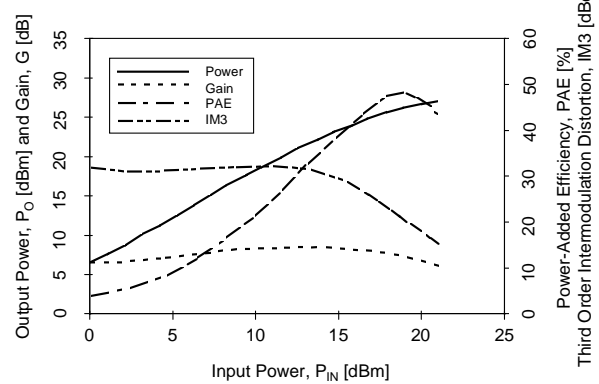


Fig. 10. Class A-B common-emitter two-tone power sweep of SiGe BJT at $V_c=7V$, $f=1.88\text{GHz}$. At $\text{IM3}=30\text{dBc}$, the device achieves a $\text{PAE}=37\%$, a significant improvement over a conventional Si BJT, which achieves roughly 25% PAE at $\text{IMR}=30\text{dBc}$ [4].

CONCLUSION:

This work has shown that SiGe BJTs are a viable technology for power applications at 1.88GHz. Class A-B biased common base parts demonstrated $> 1\text{W}$ output power with a power gain $> 15\text{dB}$, and a power-added efficiency $> 50\%$. Two-tone common-emitter measurements have demonstrated a $\text{PAE}=37\%$ at an $\text{IM3}=30\text{dBc}$ and $\text{PEP}=29\text{dBm}$. These results rival the performance of GaAs FET's and HBT's at this frequency.

REFERENCES:

- [1] D. C. Ahlgren, et al. "Manufacturability demonstration of an integrated SiGe HBT technology for the analog and wireless marketplace, *IEDM Digest*, 1996.
- [2] A. Schuppen, et al. "1-W SiGe power HBT's for mobile communication", *IEEE Micro. and Guid. Wave Lett.*, vol. 6, pp. 341-343 (1996).
- [3] A Schuppen, et al., "SiGe-technology and components for mobile communication systems," *Proc. IEEE BCTM*, pp. 130-133, 1996.
- [4] See for example, data sheet for M/A-COM PH1819-4N, or Motorola MRF6402/4.